NSRRC-J05004 (2016)

Food Hydrocolloids 56 (2016) 254–265

Contents lists available at ScienceDirect

Food Hydrocolloids

journal homepage: www.elsevier.com/locate/foodhyd

Effect of trisodium citrate on swelling property and structure of cationic starch thin film

Shing-Yun Chang, Hsi-Mei Lai*

Department of Agricultural Chetmisry, National Taiwan University, No. 1, Roosevelt Rd., Sec. 4, Taipei 10617, Taiwan

ARTICLE INFO

Article history:
Received 26 February 2015
Received in revised form
21 December 2015
Accepted 22 December 2015
Available online 24 December 2015

Keywords:
Cationic starch
Trisodium citrate
pH-sensitive
Ionic crosslinking

ABSTRACT

Effects of trisodium citrate (citrate), as an ionic crosslinker of cationic starch (CS), on swelling property of citrate-CS thin film immersing into various pH solutions were studied. The maximal turbidity of film forming solutions (FFS) indicates the most extensive ionic crosslinking of citrate to CS occurring at charge ratio (R) = 3 instead of the charge neutrality point (R = 1) due to the co-existence of electrostatic force and hydrogen bonding. The CS FFS is composed of leached amylose and unbursted swollen granules mainly occupied by amylopectin. Proved by the rheological properties of citrate-CS FFS and the microscopic images of citrate-CS thin films during swelling studies, citrate governs the pH-dependent swelling behavior within the unbursted swollen granule via ionic crosslinking either in solution or in thin films. Besides, the ionic crosslinking from citrate is able to decrease the surface hydrophilicity of CS thin film by hindering the exposure of cationic group. The small angle X-ray scattering (SAXS) patterns of swollen citrate-CS thin films are well fitted by employing the correlation length model. The rise of the exponent in low q region (n) is found to be correlated with the presence of deprotonated citrate induced aggregates, constructing a strong network against osmotic pressure, thus leading to a low water retention capacity of the thin film. Proposed nano-structure inside swollen granule from SAXS can explain the results of swelling test and microscopic images. The citrate-CS thin film can potentially serve as an active coating for pH-triggered releasing of active compounds.

© 2015 Elsevier Ltd. All rights reserved.

1. Introduction

In recent years there have been remarkable growth in the research and development on the pH regulated swelling/deswelling materials, regarding its diverse applications in drug delivery (Klinger & Landfester, 2012), sensing (Tokarev, Tokareva, Gopishetty, Katz, & Minko, 2010) and antimicrobial coating (Gensel et al., 2012). In general, pH-responsive materials are designed in the form of slab hydrogel (Chang, He, Zhou, & Zhang, 2011), microgel (Yao, Grishkewich, & Tam, 2013) and thin film. Compared to the macroscopic hydrogels, thin films have attracted more attentions due to their quick response to pH changes. The pH-responsive thin films are usually fabricated via coating processes on a solid support with advantages of the simple and effective way to prepare the switchable surfaces (Gensel et al., 2012; Kozlovskaya, Kharlampieva, Erel, & Sukhishvili, 2009). Synthetic polymers and natural polyelectrolytes containing either weak acidic or basic groups have potentials for preparing pH-responsive materials, such as polyallyamine hydrocholoride, poly(acrylic acid) (Kozlovskaya et al., 2009), alginate, chitosan, gelatin and pectin (Farris et al., 2011; Sánchez-Díaz, Becerra-Bracamontes, González-Álvarez, Cruz-Barba, & Martínez-Ruvalcaba, 2010; Tokarev et al., 2010).

pH-responsive materials show a swelling/collapse phase transition across a critical pH that is correlated to the respective pK_a or pK_b values of the weak acidic groups (e.g. carboxylic) or basic groups (e.g. amino) on the polymer, respectively. As pH > pK_a or pH < pK_b where the deprotonation or the protonation occurs, the ionization of functional groups causes the increase of internal osmotic pressure in the network, resulting in a swelling behavior. On the contrary, the absence of charges while functional groups are protonated at pH < pK_a or deprotonated at pH > pK_b results in a deswelling behavior (Klinger & Landfester, 2012; Yao et al., 2013).

In order to keep the charged polymer intact after fully swelling, chemical or ionic crosslinking is usually required. The ionic crosslinking could be simply performed by introducing two oppositely charged polymers (Farris et al., 2011; Kozlovskaya et al., 2009) or

* Corresponding author. Department of Agricultural Chemistry, National Taiwan University, No. 1, Roosevelt Rd., Sec. 4, Taipei 10617, Taiwan.
E-mail address: hmlai@ntu.edu.tw (H.-M. Lai).

http://dx.doi.org/10.1016/j.foodhyd.2015.12.029
0268-005X/© 2015 Elsevier Ltd. All rights reserved.

directly mixing small polyions into polymer solutions (Sánchez-Díaz et al., 2010). The ionic crosslinking not only can strengthen the network against osmotic pressure but also can regulate a dual swelling/deswelling behavior as pH across pK_a and pK_b (Chang et al., 2011).

Starch, the 3rd abundant biopolymer in the world, is a neutral biopolymer with many good characters, including high purity, reasonable price, biodegradability and biocompactibility. As native starch is heated in excess water above its gelatinization temperature, usually 60–70 °C for cereal starches, the starch granule swells and amylose migrates out of the granule and the gelation or pasting of starch occurred when the temperature was lowered. The characteristics of starch gels and pastes are a function of the nature of continuous phase (a three-dimensional network of soluble amylose and amylopectin molecules joined by junction zones), the nature of discontinuous phase (granule ghosts and fragments), and interactions between the two phases. In order to have a good pH-regulated behavior of starch-based material, maleic acid (Xiao & Fang, 2009) and carboxylic acid (Wang, Li, Chen, Xin, & Yuan, 2013) as charged groups have been modified on a completely solubilized starch. Different from the previous studies, we tried to directly mix a small acidic salt into a partially gelatinized cationic starch to prepare a pH-responsive CS thin film.

The acidic salt, such as trisodium citrate, has been post-dipped on the chitosan film, which showed a high drug releasing rate at pH below 3.5 due to the weak interaction of protonated citrate and chitosan (Shu, Zhu, & Song, 2001). Actually, an adequate amount of salts in solution could be directly mixed into a polymer solution based on the charge ratio of salts and polymers (Bagaria & Wong, 2011; Sánchez-Díaz et al., 2010). It has been reported that the multivalent anions (tetrasodium EDTA and trisodium citrate) had better ability to crosslink ionically than the mono- and divalent anions (sodium acetate and disodium succinate) did on the polyallylamine (Bagaria & Wong, 2011). Sodium hexametaphosphate (3% based on chitosan) incorporated into a chitosan solution by direct-mixing, also gave chitosan film a swelling/deswelling behavior (Sánchez-Díaz et al., 2010).

In our preliminary tests, trisodium citrate demonstrated an effective ionic crosslinking toward CS thin film. Citrate-CS thin film showed a swelling/collapse transition across pH 3.0 after immersing into 0.01 M NaCl solutions with various pHs. This study provides a further investigation of the effect of citrate on the physical properties of CS as a function of charge ratio, pH and furthermore, tries to localize the distribution of citrate in CS. The purposes of this study are (1) to determine the optimal charge ratio of citrate to CS in FFS for the effective ionic crosslinking, (2) to examine the effect of citrate on the surface wettability and the swelling property of CS thin films prepared by direct mixing citrate into CS FFS, (3) to evaluate the pH-dependent swelling behavior of citrate-CS thin films, and (4) to examine the macro- and nano-scale structures of citrate-CS thin films by microscopy and SAXS. The results of this study suggest that the citrate ionically crosslinked CS thin film can be used as an active surface coating after carrying the hydrophilic active compounds, which has the pH-responsive releasing character.

2. Materials and methods

2.1. Materials

Native corn starch was received from GuTong Ltd. (Chiayi, Taiwan) with protein content of 0.06% (w/w) determined by Kjeldahl method. The cationic reagent (3-chloro-2-hydroxypropyl-trimethyl ammonium chloride, CHPTAC), trisodium citrate 2-hydrate (32320, Riedel-de Haën, Missouri, USA) which was abbreviated as citrate in the text and fluorescein isothiocyanate (FITC)-dextran (molecular weight around 20,000 g/mol) were purchased from Sigma–Aldrich Co. (Missouri, USA). Chemicals used were of analytical grade.

2.2. Preparation of cationic starch (CS)

Cationic starch was prepared according to the method reported by Kuo and Lai (2007) with some modifications. Native corn starch (30 g) was suspended in 33 mL of 0.1 M NaOH, followed by adding 100 g CHPTAC with the pH 12 adjusted by using 5 N NaOH. The pH of the mixture was adjusted to 11 with 2 N NaOH, and then the mixture solution was diluted with 1 mM NaOH to the total volume of 333 mL. The cationization reaction of starch slurry was carried out in a 40 °C water bath for 24 h with continuously stirring (200 rpm). After reaction, an equivalent volume of 95% ethanol was added to precipitate the cationic corn starch. Ethanol precipitation has been widely used in recovering the granular cationic starch (Manelius, Nurmi, & Bertoft, 2000) and the gelatinized cationic starch (Khalil, Farag, & Hashem, 1993) from the reaction mixture. The precipitates were then collected by the centrifugation (10,000 × g, 10 min) at 4 °C. The precipitates were resuspended with 100 mL of 63% ethanol and neutralized with 4.8 N HCl. The neutralized cationic starch was repeatedly washed with 100 mL of 63% ethanol by either centrifugation or filtration until the conductivity of washing solution was below 10 μS/cm, at which most NaCl were removed. The absence of NaCl was confirmed by $AgNO_3$ test. The cationic starch was oven-dried at 40 °C for 1 day with the final moisture content of 13.35% before uses.

The number of cationic groups on CS was obtained by subtracting the contents of nitrogen in native corn starch from that in CS, in which the contents of nitrogen were determined by using Kjeldahl method (AACC 46-12). The degree of substitution (DS) of CHPTAC on starch was 0.12 that was calculated following the equation (1).

$$DS = \frac{(162.15 \times \%\ \text{nitrogen})}{1401 - (151.64 \times \%\ \text{nitrogen})} \quad (1)$$

where, 162.15 is the average molecular weight of anhydroglucose unit; 1401 is the 100 times of the atomic weight of nitrogen; and 151.64 indicates the molecular weight of the substituted, chloride free of CHPTAC group.

2.3. Preparation of film forming solution (FFS)

For FFS preparation, a stock CS slurry (0.4%, w/v) was partially gelatinized at 70 °C under continuously stirring (150 rpm) for 10 min, then stood at room temperature until bubbles escaped. The mixtures, containing well mixed CS stock solution (1 mL) and citrate stock solution (0–4 mM), were equilibrated at room temperature for 6 h at least to allow citrate diffusing among CS. For turbidity measurements, the FFS containing 0.2% (w/v) CS and 0–2 mM citrate were prepared. Only 0–0.6 mM citrate in 0.2% (w/v) CS FFS were prepared for film casting.

2.4. The constituents of CS FFS

After adding NaCl, the repulsive force among cationic groups of CS can be screened out and the CS FFS could be separated into supernatant and precipitate by centrifugation. Thus, the supernatant (1.7 mL) and precipitate (0.3 mL) were obtained by centrifuging 2 mL of CS FFS (0.2%, w/v) containing 0.05 M NaCl at 2180 × g for 10 min. The iodine-stained (0.2% I_2 in 2% KI) supernatant and precipitate were observed by using the optical microscopy (ECLIPSE

E600W POL, Nikon, Tokyo, Japan). Total starch content (%, on dry basis) of supernatant and precipitate were determined by using phenol-sulfuric method.

For λ_{max} measurements, the starch content of supernatant and precipitate should be adjusted to be the same (0.38 mg/mL) for comparison. Thus, the dried supernatant and precipitate were individually dissolved in the desirable amount of 0.5 M NaOH, incubated in water bath (85 °C, 10 min), followed by dilution and neutralization with 0.5% trichloroacetic acid. Finally, the iodine reagent (0.2% I_2 in 2% KI) was added into the solution and the scan of full spectrum from 500 to 700 nm was determined by using a spectrometer (UV-1700, SHIMADZU, Kyoto, Japan) after standing the solution for 20 min in the dark.

2.5. Turbidity measurement

The interaction between polycations and small polyanions is usually determined by the measurements of their turbidity as a function of small polyanion content (Han, Cheng, Wang, & Wei, 2012). The turbidity of FFS was examined as a function of the charge ratio (R), which is the ratio of total positive charges of CS to the total negative charges of divalent citrate species. The R was used to evaluate the interaction of citrate and CS dominated by electrostatic attraction. Two protons of citrate are supposed to be deprotonated at working pH around 6 because pK_a of trisodium citrate are 3.14, 4.77, and 6.39 (Murthy, Rana, & Wong, 2006). The absorbance of the upper layer of FFS (containing 0.2% CS and 0–2 mM citrate) with the R ranging from ∞ to 0.3 was measured at the wavelength of 420 nm. The turbidity was reported as 100–%T, where %T stands for the percentage of transmittance.

2.6. Rheological property measurement

The effect of citrate concentration on CS structure in both protonated and deprotonated states could be evaluated by the rheological property of FFS. In this study, the concentrated FFS within the same range of R by doubling amounts of CS (0.4%, w/v) and citrate (0–1.2 mM) were prepared for the flow property measurement because the FFS used for film casting (0.2% CS, w/v) was too dilute to obtain a reproducible shear viscosity determined by using a rheometer (DHR-1, TA instrument, New Castle, England). To observe the effect of protonated and deprotonated citrate on FFS under the same ionic strength, 20 μL of 1 M HCl and 1 M NaCl was respectively added into FFS to make 2 mL of FFS with pH = 2.0 and 5.5 (ionic strength = 0.01 M). The concentrated FFS was carefully loaded within a steel plate (60 mm diameter) and a Peltier plate with a gap of 1 mm, then equilibrated at 25 °C for 2 min before the steady shear flow measurement. Shear viscosity (η) was recorded in the range of shear rate ($\dot{\gamma}$) from 0.001 to 1000 s^{-1} in triplicate. To compare the structural changes of CS, the curves were fitted with Carreau–Yasuda equation (equation (2)), where η represents the shear viscosity; η_0 and $\dot{\gamma}$ are the zero-shear viscosity and shear rate, respectively; K is a relaxation time constant; n is the negative of the power-law slope. The best fitting curve was obtained with excel which yielded a least sum of mean square error (Sum-MSE) between the fitted and experimental data.

$$\eta = \eta_\infty + \frac{\eta_0 - \eta_\infty}{\left[1 + (K\dot{\gamma})^2\right]^{\frac{1-n}{2}}} \tag{2}$$

2.7. Preparation of CS and citrate-CS thin films

Two milliliters of FFS containing 0.2% (w/v) CS and 0–0.6 mM citrate (R = ∞–1) were casted on a polystyrene covered disc (37 mm (ID), IWAKI 3000-035, ASAHI Co., Ltd., Tokyo, Japan) for CS and citrate-CS thin films preparation. The casted FFS was dried at 40 °C/54% RH for 3 h and a thin film with the thickness about 3.5 μm was formed. To simulate the further application in the form of surface coating, final dried thin films were kept on the disc without detaching. Both CS and citrate-CS thin films were stored at 54% RH for 1 day before the following swelling studies.

2.8. Wettability and surface free energy

The contact angle measurements were carried out by the sessile drop method with a contact angle meter (FTA 125, First Ten Angstroms Inc., Portsmouth, UK). The values of surface free energy (γ_L^T), along with its dispersive (γ_L^d), and polar components (γ_L^p) of test liquids were taken from the literature (Angellier, Molina-Boisseau, Belgacem, & Dufresne, 2005). A small drop (10 μL) of two different standard liquids, distilled water ($\gamma_L^T = 72.8$ mN/m, $\gamma_L^d = 21.8$ mN/m, $\gamma_L^p = 51$ mN/m), and formamide ($\gamma_L^T = 58$ mN/m, $\gamma_L^d = 39$ mN/m, $\gamma_L^p = 19$ mN/m), was placed on the thin film surface at 25 °C. The contact angle of thin film at 3 min was recorded from at least five measurements. Surface free energy (γ_S^T), and its dispersive (γ_S^d), and polar components (γ_S^p) of thin films were estimated by the Owens-Wendt method (Equations (3) and (4)) (Owens & Wendt, 1969).

$$\gamma_S^T = \gamma_S^d + \gamma_S^p \tag{3}$$

$$\gamma_S^T(1 + \cos\theta) = 2\left(\sqrt{\gamma_S^d\gamma_L^d} + \sqrt{\gamma_S^p\gamma_L^p}\right) \tag{4}$$

2.9. Water retention capacity determination

The kinetic swelling study of CS thin film (R = ∞) was determined by immersing the CS casted disc in 250 mL of 0.01 M NaCl solution at room temperature. The immersed CS casted disc was taken out at a given time and the excess water was removed with tissue paper before weighing. After subtracting the weight of disc, the water retention capacity (WRC, g/g) of thin film at a given time (t) was calculated by equation (5), where W_t is the weight of swollen thin film at time t, and W_d (as is) is the original weight of equilibrated thin film.

$$\text{Water retention capacity(WRC, } g/g) = \frac{W_t - W_d}{W_d} \tag{5}$$

Since the time required for reaching the equilibrium water retention capacity of CS film (R = ∞) is within the first 2 min, the 2-min immersion is chosen for the following swelling behavior studies. To investigate the pH-regulated swelling behavior, the CS and citrate-CS thin films on the discs were immersed into different pH solutions (pH 2–11, adjusted with 1 M HCl and 1 M NaOH) with a fixed ionic strength (0.01 M) adjusted with 1 M NaCl. Additionally, to evaluate the salt effect at a fixed pH, WRC of CS (R = ∞) and citrate-CS thin films (R = 2) immersing into pure water and 0.01, 0.03, 0.05 and 0.1 M NaCl for 2 min were determined.

2.10. Optical and fluorescence microscopic observation

To investigate the dimensional changes of swollen granules on

CS (R = ∞) and citrate-CS (R = 2) thin films during immersion process by means of the fluorescence microscopic images, 0.02 mg/mL FITC-dextran was added into 250 mL immersion solution (0.01 M NaCl, pH 5.5). The fluorescence image was immediately taken by using a fluorescence microscope (ECLIPSE E600W POL, Nikon, Tokyo, Japan) after immersion for 30, 60, 120 and 300 s, respectively. The average diameter of swollen CS granules was calculated with Image J software (National Institutes of Health, Maryland, USA) from 20 swollen granules at least on each fluorescence microscopic image. Meanwhile, another set of CS (R = ∞) and citrate-CS (R = 3–1) thin films immersed into swelling test solutions (pH 5.5 and pH 3.0), additionally containing 0.02% I_2 and 0.05% KI, were observed under an optical microscope (ECLIPSE E600W POL, Nikon, Tokyo, Japan) after 2 min of immersion.

2.11. Small angle X-ray scattering (SAXS) measurement

The SAXS measurements were conducted at beamline 23A1 of the National Synchrotron Radiation Research Center (NSRRC, Hsinchu, Taiwan). The swollen thin film after swelling test was scratched off from the disc and then filled into a solution cell covered with kapton films on both sides. The samples were examined in a transmission mode. The sample path length of X-ray scattering was about 2.5 mm. Data were collected in synchrony with a Pilatus 1M–F area detector with a 10 keV beam (wavelength λ = 1.2410 Å). The sample-to-detector distance was approximate 4 m to cover a wide range of scattering wave vector q, ranging from 0.005 to 0.2 $Å^{-1}$. Where $q = 4\pi\sin\theta\lambda^{-1}$ and 2θ corresponds to scattering angle. Silver behenate was used for calibrating the q values of SAXS data. All data were further corrected for background scattering and transmission loss. The SAXS patterns were fit to the correlation length model (equation (6)) where A/q^n, describes the Porod scattering from the gel network in low q region, whereas the second term, $C/[1+(qL)^m]$, is a Lorentzian function describing the high q scattering. The optimal fitting was performed by employing the Igor Pro 6.11 program package provided by NIST (National Institute of Standard and Technology) Center for Neutron Research (Gaithersburg, MD, USA). The two multiplicative factors A and C, the incoherent background B, and the two exponents n and m are used as fitting parameters. The final parameter L is a correlation length. These empirical functional forms for SAXS data have been successfully applied to characterize diverse hydrogels (Hule, Nagarkar, Hammouda, Schneider, & Pochan, 2009).

$$I(q) = A/q^n + C/[1+(qL)^m] + B \quad (6)$$

3. Results and discussion

3.1. Constituents of CS FFS

Identifying the constituents of CS FFS is important in the understanding of film forming mechanism and swelling behavior of the casted thin films. By screening the charges on CS with NaCl, the leached amylose can be observed in the supernatant according to the dark blue complexes formed by amylose and iodine (Fig. 1(a)). While, the brown swollen granules can be only found in the precipitate (Fig. 1(b)) after centrifugation. It is suggested that almost all amount of amylose (24.4% on starch basis) is leached out and dissolved in the supernatant, which forms the continuous phase of FFS. While, almost all amount of amylopectin (75.6% on starch basis) is retained in the unbursted swollen granules, which can be collected in the precipitate. This can be further evidenced by their λ_{max} measurements (Fig. 1, insets).

3.2. Charge ratio (R)

The interaction of two compounds with opposite charges in a mixture is usually detected by the changes of its turbidity, where the higher turbidity expresses a stronger association of polymer chains due to the extensive ionic crosslinking (Han et al., 2012). The significant increase of turbidity usually occurs near the charge neutrality point at which the opposite charges are stoichiometrically equivalent. The dependence of FFS turbidity on the citrate concentration and the corresponding R is shown in Fig. 2. As the citrate concentration below 0.04 mM (R≥15), the turbidity keeps nearly a constant, indicating no association between citrate and CS (Fig. 2, white region). Once citrate concentration is above 0.04 mM, the turbidity increases and a maximum turbidity can be observed at 0.2–0.3 mM citrate (R = 3–2). Beyond the maximum turbidity a sharp decrease of turbidity at 0.4 mM citrate (R = 1.5) is found, where the turbidity is even lower than that of citrate-free FFS. A phase transition can be concluded from the turbidity results of citrate-CS FFS varying with citrate concentrations. The onset of ionic crosslinking is near 0.04 mM citrate (R = 15) and the CS chains begin to be associated. The most extensive ionic crosslinking occurs around 0.2–0.3 mM citrate (R = 3–2) without phase separation (Fig. 2, grey region). Above 0.3 mM citrate (R < 2), the aggregated CS precipitates gradually, and thus the upper layer turns into a polymer-poor and clear domain (Fig. 2, dark region).

In this study, the charge neutrality point of citrate-CS FFS occurring at R = 3–2 instead of R = 1 is attributed to the non-negligible amount of trivalent citrate and hydrogen bonding between citrate and CS. According to the results of turbidity measurements, citrate performs effectively ionic crosslinking with a concentration more than 0.2 mM (R ≤ 3). Thus, 0.2, 0.3, 0.5, and 0.6 mM citrate (R = 3, 2, 1.2, and 1) across the cloudy region (Fig. 2, grey region) and phase separated region (Fig. 2, dark region) were chosen for the citrate-CS thin film preparation.

3.3. Rheological properties of FFS responsive to pH

The flow curves of 0.4% CS FFS at R = ∞ and citrate-CS FFS at R = 3, 2, 1.2, and 1, which were prepared with either 0.01 M NaCl (pH = 5.5) or 0.01 M HCl (pH = 2.0) solution, are shown in Fig. A1. All viscosity profiles of CS and citrate-CS FFS show shear-thinning behavior at the intermediate shear rate while the Newtonian behavior (shear rate independent viscosity) is shown at extra-low and high shear rate. As shown in Fig. A1, the viscosity profiles can be well fitted with the Carreau–Yasuda model (Liu, Morishima, & Winnik, 2002) and the parameters derived from the fitting curves are summarized in Table 1, where K (the relaxation time constant) is equal to the inverse of critical shear rate at the onset of shear thinning and n shows the steepness of the power-law region. Without citrate, there is no significant change on η_0 of CS FFS at pH 5.5 and 2.0, but a larger K could be found in CS FFS at pH 2.0. At the same pH conditions, CS FFS (R = ∞) always possesses a larger η_0 and K than the citrate-CS FFS. Increasing in the citrate concentration (decreased R) of citrate-CS FFS, both η_0 and K decrease at pH 5.5. When citrate is protonated at pH 2.0, η_0 and K of all citrate-CS FFS obviously increase to the similar values. In Carreau–Yasuda model, the increases of η_0 and K usually indicate the increase of the crosslinking density of polymer chains, resulting in a large polymer size (Liu et al., 2002).

It has been evidenced that the CS FFS contained the unbursted swollen granules mainly filled with amylopectin inside, which are located within the amylose matrix (Fig. 1). The unbursted swollen granules in starch paste have been reported displaying the microgel-like viscoelastic behavior (Evans & Lips, 1992; Yao et al., 2013). Since the viscoelastic property of FFS is dominated by the

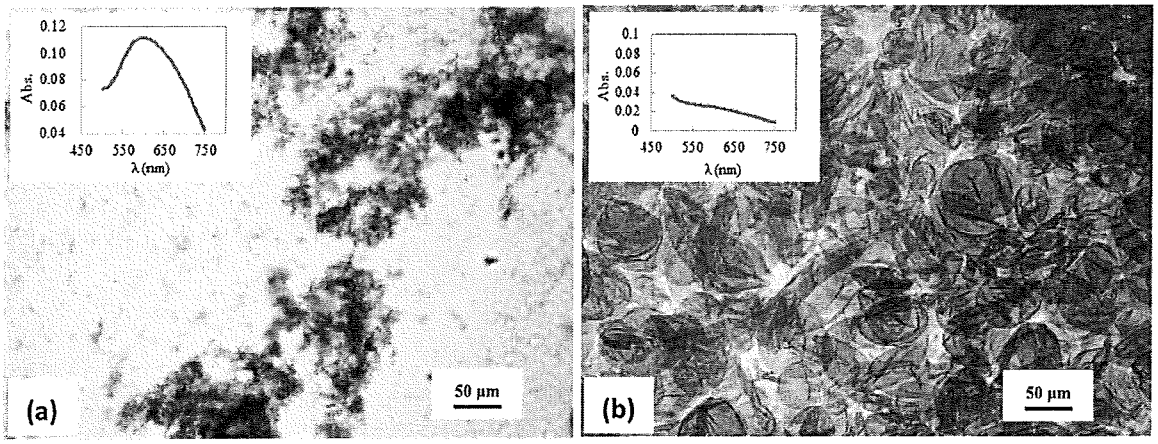

Fig. 1. The microscopic images of iodine-stained supernatant (a) and precipitate (b) separated from FFS, along with their scan of full spectra from 500 to 700 nm (insets). Scale bar = 50 μm.

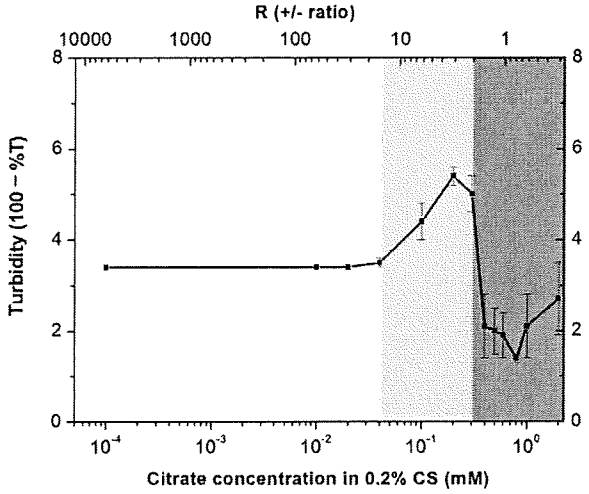

Fig. 2. Turbidity (100−%T, where %T is the percentage of transmittance) of 0.2% CS FFS depending on the citrate concentration and the calculated charge ratio (R) which is the ratio of total positive charges of CS to the total negative charges of divalent citrate species. The regions with gray and dark gray shadows indicate that the citrate interacts with CS without precipitation and with precipitation, respectively.

Table 1
The zero-shear viscosity (η_0), relaxation time constant (K) and molecular weight constant (n) derived from the fitting results of flow curves (Fig. A1) with Carreau–Yasuda model.

FFS (R)/media[a]	η_0 (Pa·s)	K	n	Sum-MSE[b] (× 10^{-3})
CS (R=∞)/pH 5.5	0.40	18	0.54	4.9
CS (R=∞)/pH 2.0	0.44	30	0.56	11
Citrate-CS (R=3)/pH 5.5	0.14	8	0.60	0.79
Citrate-CS (R=3)/pH 2.0	0.24	20	0.60	5.2
Citrate-CS (R=2)/pH 5.5	0.06	5	0.68	0.044
Citrate-CS (R=2)/pH 2.0	0.27	20	0.60	2.1
Citrate-CS (R=1.2)/pH 5.5	0.05	3	0.65	0.059
Citrate-CS (R=1.2)/pH 2.0	0.26	20	0.60	1.0
Citrate-CS (R=1)/pH 5.5	0.04	2	0.65	0.045
Citrate-CS (R=1)/pH 2.0	0.31	25	0.60	2.3

[a] FFS (R)/media expresses as the film forming solution with the charge ratio (R in parentheses) under either 0.01 M NaCl (pH = 5.5) or 0.01 M HCl (pH = 2.0) conditions.

[b] Sum-MSE: the sum of the mean square error between the experimental viscosity and the deduced viscosity with Carreau–Yasuda model.

size of swollen granules, the higher η_0 and K of CS FFS indicate the higher compactness arising from the fully swollen granules. Thus, the largest size of swollen granules in CS FFS at pH 2.0 is attributed to the largest amount of ionized quaternized amine on CS. In the presence of citrate at pH 5.5, the deprotonated citrate crosslinking CS chains result in the smaller size of swollen granules due to the limited swelling as evidenced by their small η_0 and K. At pH 2.0, more protonated citrates reduce the chance to ionically crosslink with CS chains, so the size of swollen granules in citrate-CS FFS is enlarged. Comparing to the CS FFS at pH 2.0, the incompletely recovered η_0 and K of citrate-CS FFS at pH 2.0 are attributed to the excluded volume of the protonated citrate that results in the spatial limited swelling of CS. Besides, the slight increase of n in citrate-CS FFS with R < 3 at pH 5.5 indicates that ionic crosslinking from citrate may slightly increase the molecular weight of CS (Liu et al., 2002).

3.4. Wettability, kinetic swelling properties, and morphology of CS and citrate-CS thin films

Contact angle is a basic wetting property used to evaluate the degree of surface hydrophilicity on a film or a coating (Choi, Park, Ahn, Lee, & Lee, 2002). As shown in Table 2, the CS thin film gives the lowest contact angle of a water drop, which expectedly arises from both the quaternized amine and hydroxyl group-rich surface. The contact angle of a water drop significantly increases in the presence of citrate, and becomes steady at R≤1.2. This implies that the included citrate decreases the hydrophilicity of the thin film. Depending on the changes of surface energy of CS and citrate-CS thin films, the introduction of citrate does not change the dispersive component of surface energy (γ^d) whereas the polar one (γ^p) decreases obviously. It demonstrates that citrate tends to react with the polar groups (i.e. quaternized amine) while does not provide the additional apolar groups on the thin film. Similar trends have been reported for the modified starch subtracts (Angellier et al., 2005).

In addition to the surface hydrophilicity, the swelling properties and the morphology of CS and citrate-CS thin films can further demonstrate how the ionic crosslinking constrains the affinity of CS with water. Fig. 3 shows the water retention capacity (WRC) of CS thin film (R = ∞) in 0.01 M NaCl as a function of immersion time. CS thin film absorbs water rapidly within the first 100 s (WRC = 50 g/g), after that, WRC remains around 50 g/g until 300 s, and increases to 60 g/g after immersing for 600 s. By visual inspection, CS thin

Table 2
Contact angle (°) and surface free energy (γ) of CS (R = ∞) and citrate-CS thin films (R = 3, 2, 1.2, and 1).

Thin film types	Contact angle (°)		Owens-Wendt[1]		
	Water	Formamide	γ^T (mN/m)	γ^p (mN/m)	γ^d (mN/m)
CS (R=∞)	37.02 ± 2.81[a2]	29.25 ± 1.70[a]	79.48	52.66	26.82
Citrate-CS (R=3)	46.56 ± 1.39[b]	23.78 ± 1.82[b,c]	75.42	47.87	27.55
Citrate-CS (R=2)	50.73 ± 0.75[c]	21.35 ± 1.35[c]	73.50	45.63	27.87
Citrate-CS (R=1.2)	53.08 ± 1.86[c,d]	24.58 ± 2.90[b]	72.68	44.92	27.75
Citrate-CS (R=1)	53.54 ± 1.69[d]	21.48 ± 1.21[c]	72.28	44.29	27.98

[1] γ^T: total surface free energy; γ^p: surface free energy (polar); and γ^d: surface free energy (dispersive).
[2] Means with the same letter are insignificantly different at $p < 0.05$ according to the LSD test. LSD test was performed for each solvent.

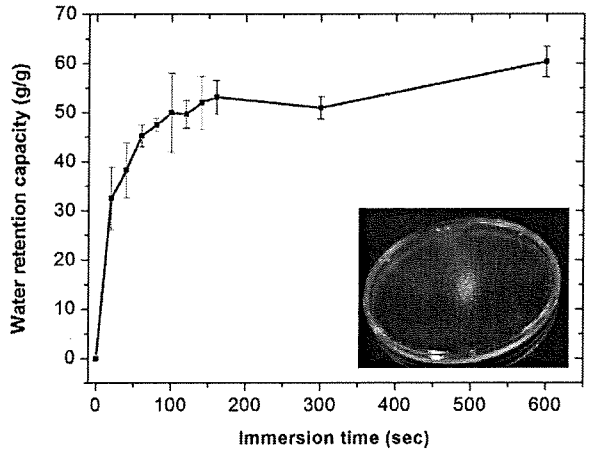

Fig. 3. The water retention capacity of CS thin film on a disc in 0.01 M NaCl solution as a function of immersion time was plotted. The picture of swollen CS thin film on the disc after the immersion for 5 min is inserted.

film could stand on the disc without dissolution in the first 300 s of immersion (Fig. 3, inset), and the thin film was not dissociated until 600 s. That is the reason why a 2-min immersion test was chosen for the further investigation of swelling behavior responsive to pH.

To simultaneously investigate the morphological changes of swollen CS granules on the thin films during immersion process, the fluorescence images of CS (R = ∞) and citrate-CS (R = 2) thin film were taken during swelling study for 30, 60, 120, and 300 s (Fig. 4(a–h)). FITC-dextran is a giant fluorescence dye with a radius around 3.3 nm. Unlike ionic dyes, neutral FITC-dextran has no screening effect toward CS chains, therefore, the size of swollen granules in thin films can be estimated during immersion process. Visualized by the absorbed FITC-dextran during swelling process, the fluorescence images of CS swollen granules with an increased degree of swelling are shown in Fig. 4. The dimensional growth of swollen granules seems proportional to the expansion of the dark region inside swollen granules of CS and citrate-CS thin film during immersion process (Fig. 4(a–d) for CS, and (e-h) for citrate-CS thin film). This indicates that the cationic group-rich inner region of the swollen granule plays a very important role on the swelling behavior.

The calculated averaged diameter of swollen granules taken from the CS thin film images is 60 μm at the first 30 s of immersion, then it swells to 90 μm after 5 min of immersion (Fig. 4(a, d, and i)). At the same immersion time, the size of swollen granules on citrate-CS thin film shows only half size of those on CS thin film (Fig. 4(e, h, and i)). For those starch granules having surface pores and connected channels (e.g. corn starch), it has been reported that the relatively intensive modification is on the surface of granule, channels and the amorphous region near interior cavity according to the diffusion pathway of cationic reagent in starch granules (Kuo & Lai, 2009; Manelius et al., 2000). Comparing to the CS thin film (Fig. 4(a–d)), the macroscopic restriction of dark region observed on citrate-CS thin film (Fig. 4(e–h)) implies that the citrate must diffuse into cationic group-rich region and interact with CS.

3.5. Swelling behavior and morphology of CS and citrate-CS thin films responsive to pH

The WRC of CS (R = ∞) and citrate-CS (R = 3, 2, 1.2, and 1) thin films in different pH solutions (ranging from 2 to 11) with ionic strength of 0.01 M are shown in Fig. 5(a). The WRC of CS thin film decreases first from pH 2 to 3, keeps a constant at pH 4–5.5, increases at pH 7, and then decreases again above pH 7 (Fig. 5(a), CS (R = ∞)). As mentioned in the rheological results in section 3.3, a complete ionization of quaternized amine resulting in a larger K at pH 2, responds to the higher WRC of CS thin film at pH 2. The increased WRC at neutral pH may result from the less dissolution of CS thin film at pH 7 and 8, comparing to that at either weak acid (pH 3–5.5) or weak base (pH 9) condition. The similar phenomenon has been reported on the native starch granules at various pH (Yusuf, Ayedun, & Logunleko, 2007). At pH 10, above the pK_a of quaternized amine (~9.8), the degree of deprotonation of quaternized amine increases, resulting in a significant shrinkage of CS swollen granules.

Once citrate is introduced into CS chains with R ≤ 2, citrate plays an important role in controlling WRC over a wide range of pH. A significant drop in WRC of citrate-CS thin film is observed as pH increases across the pK_{a1} (3.14) of citrate, while no significant changes in WRC responding to the pH ranging from 4 to 9 (Fig. 5(a), citrate-CS (R = 2, and 1.2)). In citrate-CS thin film with R = 1 by introducing more citrate (Fig. 5(a), citrate-CS (R = 1)), the pH dependent swelling behavior of citrate-CS thin film is overwhelmed by the citrate regulated swelling behavior. A similar study done by Shu et al. (2001), in which citrates played as an ionic crosslinker in chitosan film (50 mg) via post-dipping in 100 mL of 1% (w/v) citrate solution for 1 h, found the citrate-controlled ionic crosslinking present at pH 4.3–7.6, but absent at pH ≤ 3.5. In this study, the swelling behavior of CS thin film can be effectively controlled by citrate which has been directly mixed into the FFS. Quantitatively, citrate with R≤2 (i.e. > 37.5 mg/g dried CS) is required to ionically crosslink to CS. Fig. 5(b) shows the salt effect on the WRC of CS (R = ∞) and citrate-CS (R = 2) thin films. In pure water, there is a large difference in WRC up to 100 g/g between these two thin films. Increasing NaCl concentration to 0.01 M, the difference of WRC between them is diminished to 10 g/g. Above 0.03 M NaCl, WRC are around 25 g/g for both CS (R = ∞) and citrate-CS (R = 2) thin films. The WRC dependence on salt concentration is attributed to Donnan osmotic pressure inside CS swollen granules that decreases as the environmental salt concentration increases. As a result, little amount of water can diffuse into CS swollen

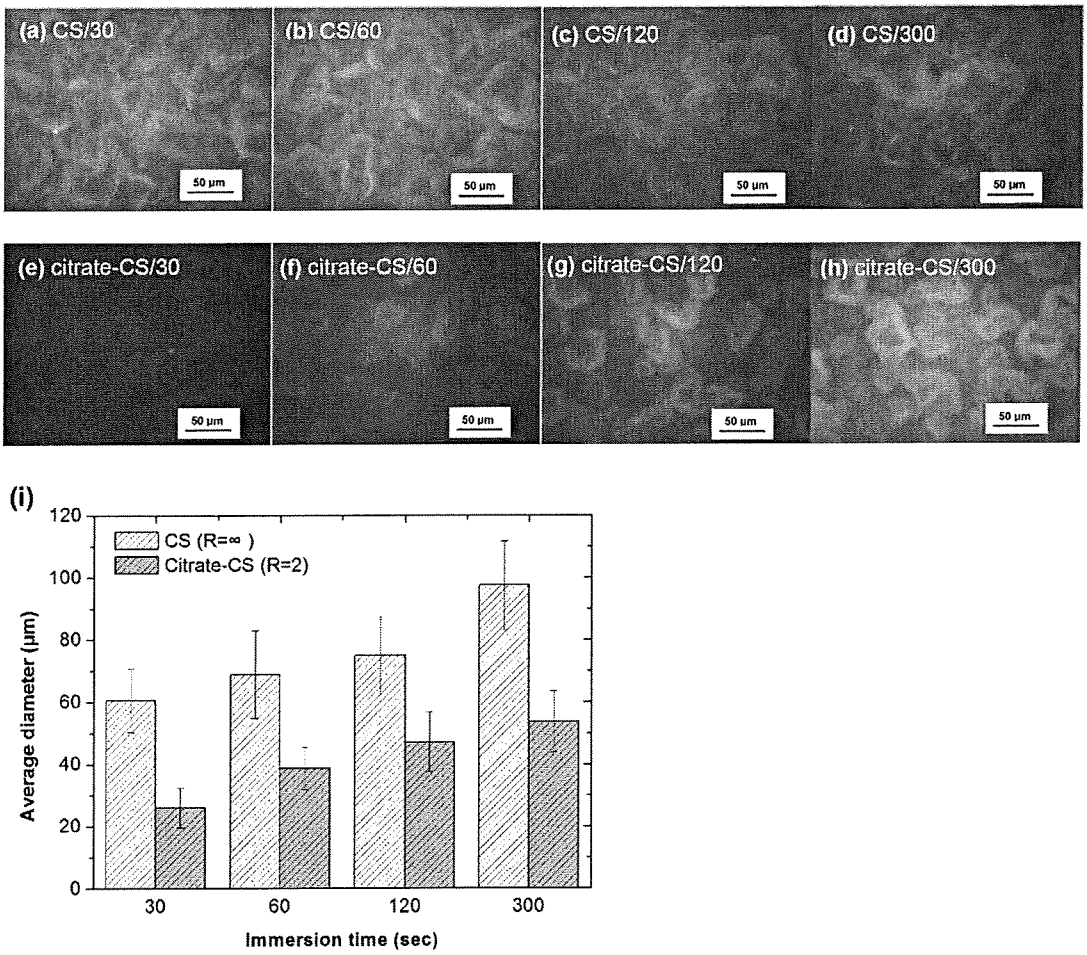

Fig. 4. The fluorescence microscopic images of CS thin film (R = ∞) and citrate-CS thin films (R = 2) which were immersed for 30 (a, e), 60 (b, f), 120 (c, g) and 300 s (d, h), respectively. The average diameter of swollen granules in CS (R = ∞) and citrate-CS thin films (R = 2) as a function of immersion time (i) were calculated from 20 granules at least on each fluorescence microscopic image. Citrate diffusing into the cationic group-rich region in the interior of swollen granules which resulted in the restricted expansion of swollen granules can be observed in the citrate-CS thin film.

granules at high salt concentration. In other words, the Cl^- screens the charged groups on CS chains, like the neutral starch chains, which are not affected by citrates any more. A similar result is reported on the hydrogels consisting of anionic and cationic cellulose that the highest swelling ratio was observed in pure water and the swelling was restricted in 0.03 M NaCl solution as well (Chang et al., 2011).

The morphological changes of swollen granules on CS (R = ∞) and citrate-CS thin films (R = 3, 2, 1.2, and 1) after WRC measurements carried out at pH 5.5 (Fig. 6(a–e)) and pH 3.0 (Fig. 6(f–j)) were investigated by optical microscopy. Here, the KI/I_2 solution is used to enhance the contrast of thin films. At pH 5.5 (Fig. 6(a–e)), the more citrates introduced in CS thin films, the smaller size of CS swollen granules can be observed due to the increase of ionic crosslinking. Loss of ionic crosslinking at pH 3.0, the limited expansion of CS swollen granules can be seen in low R (Fig. 6(f–j)). This proves that the swelling ability of citrate-CS thin film at low pH can be spatially interfered by the protonated citrate as mentioned in the rheological results (Section 3.3).

Taking into account of the pH effect, no difference in size is observed between CS thin films (R = ∞) at pH 5.5 and pH 3.0 (Fig. 6(a, f)). Once citrates are incorporated in CS thin films, the CS swollen granules are significantly shrunken at pH 5.5 (Fig. 6(b–e)) and expanded at pH 3.0 (Fig. 6(g–j)). The expansion degrees of CS swollen granules correspond well to their WRC values (Fig. 5(a) pH 3 & 5.5). This is attributed to the electrostatic interaction between the cationic groups on CS and the anionic groups of the citrates occurring inside swollen granules and this electrostatic interaction presents at pH > pK_{a1} of citrate, but loses at pH < pK_{a1}.

3.6. Nanostructure of CS and citrate-CS thin films responsive to pH

Fig. 7 shows the SAXS patterns of CS (R = ∞) and citrate-CS (R = 3, 2, and 1.2) thin films right after WRC measurements at pH 5.5 and pH 3.0. All SAXS curves can be well fitted with the correlation length model and the extracted parameters are shown in Table 3. With the aid of model fitting, the structural information can be obtained by evaluating the parameters *n*, *L* and *m*, respectively. Taking the swollen CS thin film at pH 3.0 as an example, every SAXS pattern can be roughly divided into three regions (Fig. 7(a)). In region I (below 0.015 $Å^{-1}$), a typical polyelectrolyte upturn relating to the aggregates or locally ordered domains can be found (Salamon, Aumiler, Pabst, & Vuletic, 2013). A shoulder-like peak around 0.03 $Å^{-1}$ in the middle *q* range (Region II: 0.015–0.05 $Å^{-1}$) is contributed by the correlation length, representing the spatial

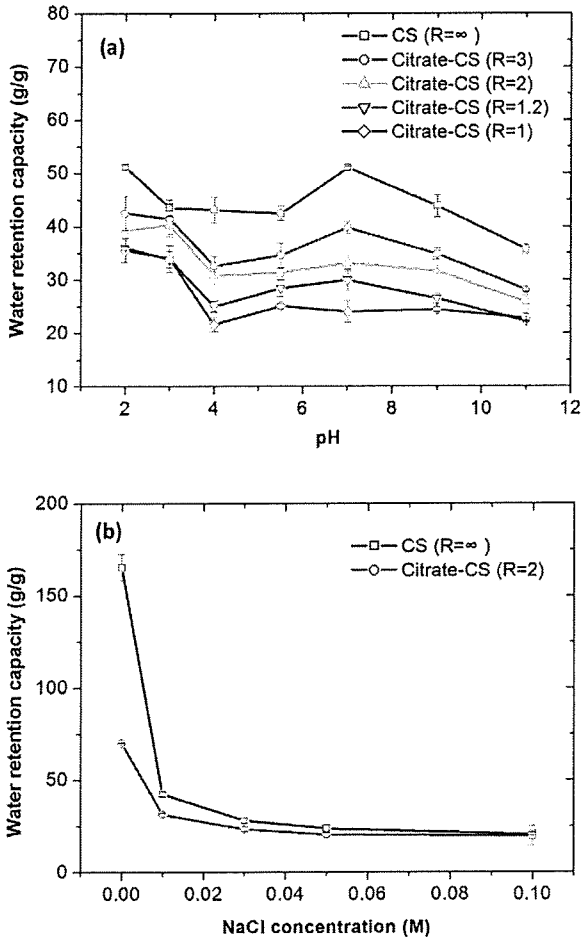

Fig. 5. pH effect (a) and salt effect (b) on the swelling behavior of CS (R = ∞) and citrate-CS thin films (R = 3, 2, 1.2, and 1 for pH effect and R = 2 for salt effect).

Doublier, & Axelos, 1995). In high q region (Region III: 0.05–0.2 $Å^{-1}$), the scattering arises from the local structure of the constructed components.

In Table 3, the low q scattering exponent (n) is attributed to the scattering from the aggregated CS chains in network with the size exceeding the resolution of SAXS measurements (>200 Å given by $2\pi/q$). Higher n found in swollen CS (R = ∞) at pH 5.5 than that at pH 3.0 indicates that the aggregates begin to form without strong repulsive force among fully charged CS chains. The higher n in the swollen citrate-CS thin films at pH 5.5 than that at pH 3.0 is contributed by the presence of the ionic crosslinking from deprotonated citrate. As citrate is protonated at pH 3.0, no longer interacting with charged CS chains, thus n decreases. The difference of n between pH 5.5 and 3.0 becomes significant as R≦2, corresponding to the amount of charged citrates needed for performing the ionic crosslinking on CS concluded from the swelling behavior study in section 3.5.

The shoulder-like peak around 0.03 $Å^{-1}$ in all SAXS patterns is resulted from the correlation length (L) within the range from 38 to 59 Å (Table 3). Comparing to the L and the n of swollen thin films at pH 3.0, a slightly larger correlation length of ~5 Å (larger L) along with the larger aggregates > 200 Å (larger n) is found in the swollen thin films at pH 5.5. Regarding to the hierarchical structure of starch, the calculated L is much smaller than the gyration radius (312 nm) of corn starch amylopectin reported by Yoo and Jane (2002). This indicates that the calculated correlation length from SAXS patterns is ascribed to the mesh size within an amylopectin molecule. As the discussion in section 3.4, the cationic reagents preferentially reacted with anhydroglucose unit on the surface of granule, channels and the amorphous regions in raw starch granules. The amylopectin clusters embedded in crystalline regions are the least reacted regions which will keep neutral and the meshes (polymer poor region) around 44 Å lie inside the neutral part of an amylopectin, according to the calculated L of swollen CS thin films (R = ∞) at pH 5.5.

As the attractive forces among amylopectin molecules are

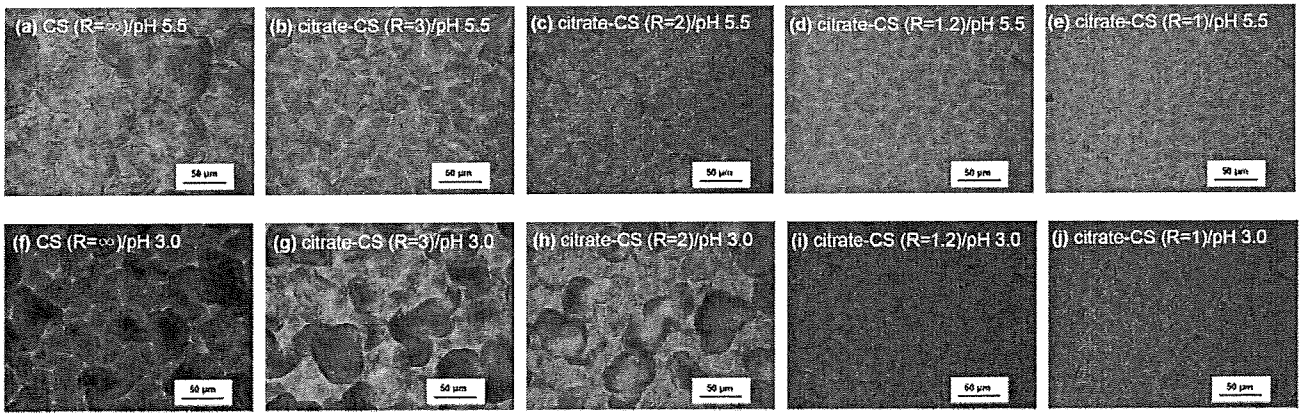

Fig. 6. The microscopic pictures of CS (a, f) and citrate-CS thin films (R = 3 (b, g), 2 (c, h), 1.2 (d, i), and 1 (e, j)) after water retention capacity measurements at pH 5.5 (a–e) and pH 3.0 (f–j), respectively. The KI/I_2 was introduced in solution to increase the contract of swollen granules for easy identification. Scale bar = 50 μm. In the presence of deprotonated citrate, the citrate-CS swollen granules are significantly shrunken at pH 5.5, while expanded as citrates are protonated at pH 3.0.

correlation of concentration fluctuations in the system. In the semi-diluted condition of polymer just like the starch concentration in the swollen CS and citrate-CS thin films, the correlation length is recognized as the mesh size of network (Turquois, Rochas, Taravel, introduced by the existence of citrates in CS thin film at pH 5.5, the aggregation occurs (large n), responding to the enlargement of mesh size (large L) within a dragged amylopectin molecule. The contrary findings are as expected that the mesh size decreased due

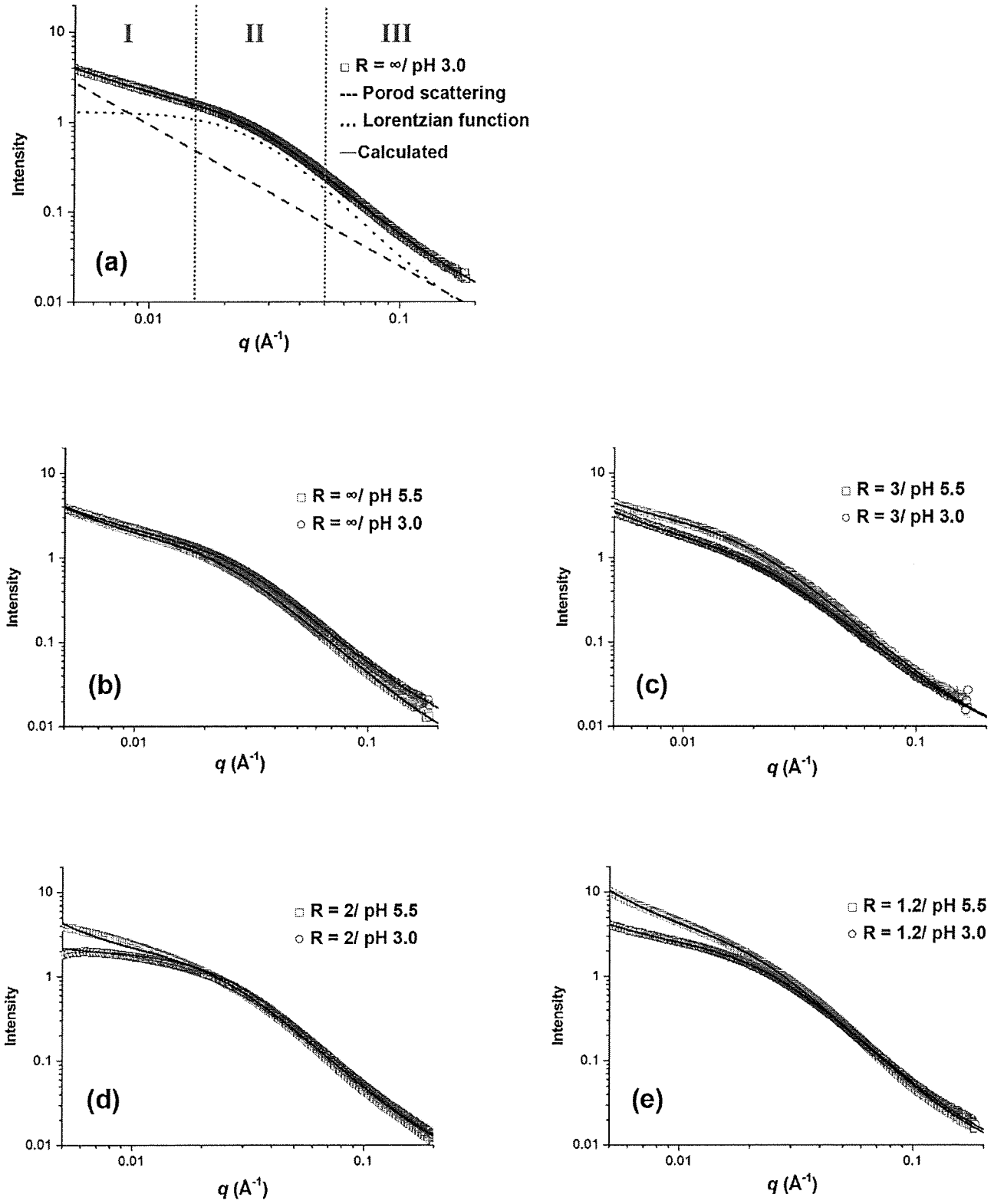

Fig. 7. Observed (open squares) and calculated (solid line) SAXS patterns of CS (a) after water retention capacity measurement in pH 3.0 solution. The dashed lines indicate two contributions from the scattering of network in nano-scale, by employing the Porod scattering (dash line) and the Lorentzian function (dot line); Observed (open squares) and calculated (solid line) SAXS profiles of CS (b) and citrate-CS thin films with R = 3 (c), R = 2 (d), and R = 1.2 (e) after swelling tests in pH 3.0 and pH 5.5 solutions. The main structural change responsive to pH in citrate-CS thin films relates to if large aggregates formed or not. Aggregates will contribute a sharp slope of SAXS curve in the low *q* region. The fitted parameters are shown in Table 3.

Table 3
Fit parameters for the correlation length model applied to SAXS data (Fig. 7) of swollen CS (R = ∞) and citrate-CS thin films (R = 3, 2, and 1.2) in pH 5.5 and pH 3.0

Swollen thin film (R)/media[a]	*n*	*L* (Å)	*m*
CS (R=∞)/pH 5.5	1.87	44	2.58
CS (R=∞)/pH 3.0	1.57	39	2.81
Citrate-CS (R=3)/pH 5.5	1.99	59	2.44
Citrate-CS (R=3)/pH 3.0	1.95	54	2.33
Citrate-CS (R=2)/pH 5.5	2.20	45	2.54
Citrate-CS (R=2)/pH 3.0	1.75	41	2.62
Citrate-CS (R=1.2)/pH 5.5	2.13	52	2.70
Citrate-CS (R=1.2)/pH 3.0	1.80	46	2.50

[a] Swollen thin film (R)/media expresses as the thin film with the charge ratio (R in parentheses) under either pH = 5.5 or pH = 2.0.

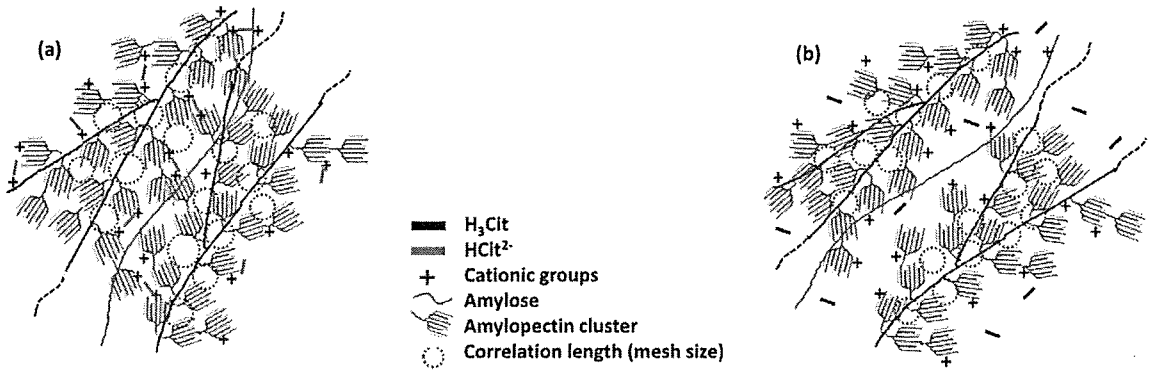

Fig. 8. Schematic illustrations proposed for the nano-structure of swollen granules on citrate-CS thin film (R = 1.2) responsive to pH 5.5 (a) and pH 3.0 (b). The mesh of network is suggested among the clusters within the amylopectin molecules with the least modification and the ionic crosslinking of deprotonated citrate on CS chains causes the formation of aggregates among CS molecules.

to the strong repulsive force among the amylopectin molecules as the result of the fully ionized quaternized amine in CS thin film at pH 3.0.

The signal in high q region (0.05–0.2 $Å^{-1}$) is the scattering from the local structure within an amylopectin (~20–5 Å given by $2\pi/q$). Here, m around 2.35 is attributed to the highly diffused interface of mesh within amylopectin. Similar m derived from the SAXS patterns was reported on the swollen microbial cellulose films (Koizumi, Tomita, Kondo, & Hashimoto, 2009).

3.7. Proposed schematic illustration of nano-structure of citrate-CS swollen granules

Citrate is demonstrated playing an important role on pH-dependent swelling behavior in citrate-CS thin films. The swelling of unbursted swollen granules is under the control of state of citrate. Fig. 8(a) and (b) are the proposed schematic illustrations of nano-structure of citrate-CS swollen granules (R = 1.2) responsive to pH 5.5 and 3.0 based on the SAXS results, respectively. Since CHPTAC diffuses along amorphous regions during modification, the outer side-chains, some branching points of amylopectin and amylose are easily substituted (Kuo & Lai, 2009; Manelius et al., 2000). The correlation length L, corresponding to the mesh size, around 50 Å (blue (in the web version) dashed circles in Fig. 8) are situated inside each amylopectin molecule where limited cationic groups are substituted. At pH 5.5, the deprotonated citrates (green (in the web version) bars in Fig. 8(a)) ionically crosslinked the charged groups on CS molecules (mainly amylopectin) and formed large aggregates, which is indicated by a higher exponent (n) in SAXS patterns (Table 3). The aggregated CS chains construct a strong network in thin films against osmotic pressure during swelling tests (Fig. 5(a), R = 1.2). At pH 3.0, the smaller n is observed because the protonated citrate (blue bars in Fig. 8(b)) is unable to interact with CS chains and results in a weak network. Without restriction of citrate at pH 3.0, the strong repulsive force from CS chains slightly reduced the mesh size inside amylopectin.

4. Conclusions

Through a mild cationization, partial gelatinization, and casting process, leached amylose offers CS a film forming ability and the unbursted swollen granule provides CS a microgel-like swelling behavior. The addition of citrate with R ≤ 2 promises either citrate-CS FFS or thin film an evident pH-responsive swelling behavior. The ionic crosslinking between citrate and cationic group decreases the surface hydrophilicity of thin films as well. The pH-regulated swelling/collapse transition is dominated by the expansion degree of the unbursted swollen granule, occurring near pK_{a1} of citrate (3.14). Mostly, citrate performs ionic crosslinking in the interior of swollen granule where cationic group is rich, i.e. the outer rim and the amorphous regions of amylopectin in the unbursted swollen granule. Within a swollen granule, deprotonated citrate ionically crosslinking CS leads to the aggregates in nano-scale (>200 Å, observed in SAXS pattern). The aggregated CS chains result in the thick network that provides the capability against osmotic pressure at pH > 3.

In this study, a novel pH-responsive starch-based thin film is prepared by directly mixing trisodium citrate into a partially gelatinized cationic starch. It can be used as the active coating material and coated on the surface of a substrate or a base film for the purposes of product protection, nutrient enrichment, deterioration sensor etc. In this case, a hydrophilic active compound can be simply introduced into FFS to prepare a citrate-CS thin film with the character of pH-triggered releasing in food systems. In addition, some other active compounds and drugs with multivalent negative charges are worth trying in this CS-thin film instead of trisodium citrate used in current FFS. Different pH threshold for triggering the release can be expected depending on the specific ionic crosslinker.

Acknowledgments

This work was supported by the grant NSC101-2313-B-002-067 from Ministry of Science and Technology, Taipei, Taiwan.

Appendix

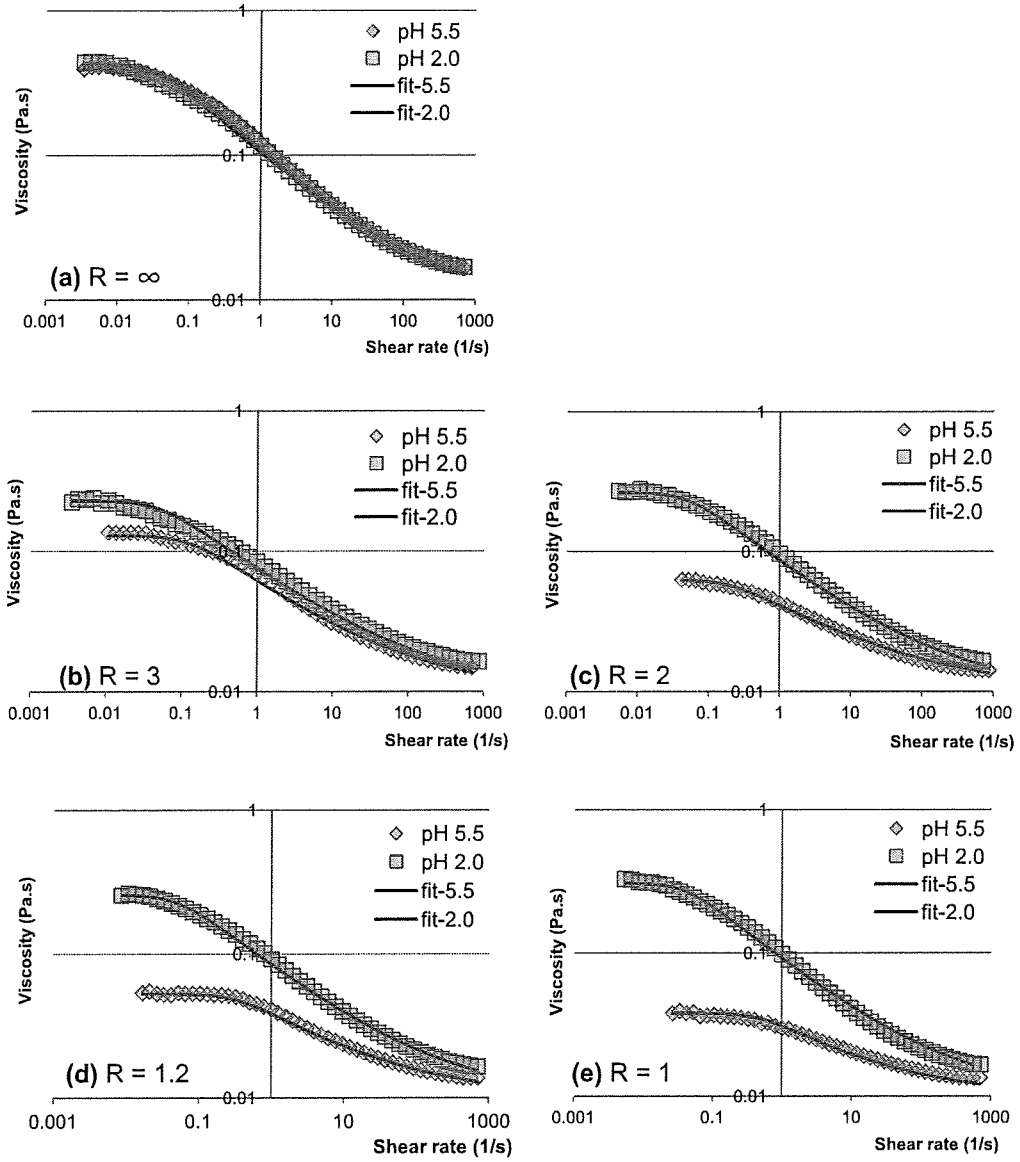

Figure A.1. The flow curve of 0.4% CS FFS at R = ∞ (a) and citrate-CS FFS at R = 3 (b), 2 (c), 1.2 (d), 1 (e), prepared with either 0.01 M NaCl (pH = 5.5) or 0.01 M HCl (pH = 2.0) solution. Black lines represent the fitting curves with Carreau-Yasuda model by the fitted parameters shown in Table 1. A drop of viscosity indicates the low compactness of the swollen granules in citrate-CS FFS (R = 2, 1.2 and 1) with limited expansion at pH 5.5.

References

AACC. (2000). *Approved methods of the AACC, 10th ed. Method 46–12.* St. Paul, Minnesota: American Association of Cereal Chemists, Inc.

Angellier, H., Molina-Boisseau, S., Belgacem, M. N., & Dufresne, A. (2005). Surface chemical modification of waxy maize starch nanocrystals. *Langmuir, 21,* 2425–2433.

Bagaria, H. G., & Wong, M. S. (2011). Polyamine-salt aggregate assembly of capsules as responsive drug delivery vehicles. *Journal of Materials Chemistry, 21,* 9454–9466.

Chang, C., He, M., Zhou, J., & Zhang, L. (2011). Swelling behaviors of pH- and salt-responsive cellulose-based hydrogels. *Macromolecules, 44,* 1642–1648.

Choi, W. Y., Park, H. J., Ahn, D. J., Lee, J., & Lee, C. Y. (2002). Wettability of chitosan coating solution on 'Fuji' apple skin. *Journal of Food Science, 67,* 2668–2672.

Evans, I. D., & Lips, A. (1992). Viscoelasticity of gelatinized starch dispersions. *Journal of Texture Studies, 23,* 69–86.

Farris, S., Schaich, K. M., Liu, L. S., Cooke, P. H., Piergiovanni, L., & Yam, K. L. (2011). Gelatin-pectin composite films from polyion-complex hydrogels. *Food Hydrocolloids, 25,* 61–70.

Gensel, J., Borke, T., Pérez, N. P., Fery, A., Andreeva, D. V., Betthausen, E., et al. (2012). Cavitation engineered 3D sponge networks and their application in active surface construction. *Advanced Materials, 24,* 985–989.

Han, J., Cheng, F., Wang, X., & Wei, Y. (2012). Solution properties and microstructure of cationic cellulose/sodium dodecyl bezene sulfonate complex system. *Carbohydrate Polymers, 88,* 139–145.

Hule, R. A., Nagarkar, R. P., Hammouda, B., Schneider, J. P., & Pochan, D. J. (2009). Dependence of self-assembled peptide hydrogel network structure on local fibril nanostructure. *Macromolecules, 42,* 7137–7145.

Khalil, M. I., Farag, S., & Hashem, A. (1993). Preparation and characterization of some cationic starches. *Starch/Stärke, 45,* 226–231.

Klinger, D., & Landfester, K. (2012). Stimuli-responsive microgels for the loading and release of functional compounds: fundamental concepts and applications. *Polymer, 53,* 5209–5231.

Koizumi, S., Tomita, Y., Kondo, T., & Hashimoto, T. (2009). What factors determine hierarchical structure of microbial cellulose – interplay among physics,

chemistry and biology. *Macromolecular Symposia, 279*, 110–118.
Kozlovskaya, V., Kharlampieva, E., Erel, I., & Sukhishvili, S. A. (2009). Multilayer-derived, ultrathin, stimuli-responsive hydrogels. *Soft Matter, 5*, 4077–4087.
Kuo, W.-Y., & Lai, H.-M. (2007). Changes of property and morphology of cationic corn starches. *Carbohydrate Polymers, 69*, 544–553.
Kuo, W.-Y., & Lai, H.-M. (2009). Effects of reaction conditions on the physico-chemical properties of cationic starch studied by RSM. *Carbohydrate Polymers, 75*, 627–635.
Liu, R. C. W., Morishima, Y., & Winnik, F. M. (2002). Rheological properties of mixtures of oppositely charged polyelectrolytes. A study of the interactions between a cationic cellulose ether and a hydrophobically modified poly[sodium2-(acrylamido)-2-methylpropanesulfonate]. *Polymer Journal, 34*, 340–346.
Manelius, R., Nurmi, K., & Bertoft, E. (2000). Enzymatic and acidic hydrolysis of cationized waxy maize starch granules. *Cereal Chemistry, 77*, 345–353.
Murthy, V. S., Rana, R. K., & Wong, M. S. (2006). Nanoparticle-assembled capsule synthesis: formation of colloidal polyamine-salt intermediates. *The Journal of Physical Chemistry B, 110*, 25619–25627.
Owens, D. K., & Wendt, R. C. (1969). Estimation of the surface free energy of polymers. *Journal of Applied Polymer Science, 12*, 1741–1646.
Salamon, K., Aumiler, D., Pabst, G., & Vuletic, T. (2013). Probing the mesh formed by the semirigid polyelectrolytes. *Macromolecules, 46*, 1107–1118.
Sánchez-Díaz, J. C., Becerra-Bracamontes, F., González-Álvarez, A., Cruz-Barba, L. E., & Martínez-Ruvalcaba, A. (2010). Effect of sodium hexametaphosphate concentration on the swelling and controlled drug release properties of chitosan hydrogels. *Journal of Applied Polymer Science, 117*, 3595–3600.
Shu, X. Z., Zhu, K. J., & Song, W. (2001). Novel pH-sensitive citrate cross-linked chitosan film for drug controlled release. *International Journal of Pharmaceutics, 212*, 19–28.
Tokarev, I., Tokareva, I., Gopishetty, V., Katz, E., & Minko, S. (2010). Specific biochemical-to-optical signal transduction by responsive thin hydrogel films loaded with noble metal nanoparticles. *Advanced Materials, 22*, 1412–1416.
Turquois, T., Rochas, C., Taravel, F.-R., Doublier, J. L., & Axelos, M.-A.-V. (1995). Small-angle X-ray scattering of k-carrageenan based systems: sols, gels, and blends with carob galactomannan. *Biopolymers, 36*, 559–567.
Wang, Z., Li, Y., Chen, L., Xin, X., & Yuan, Q. (2013). A study of controlled uptake and release of anthocyanins by oxidized starch microgels. *Journal of Agricultural and Food Chemistry, 61*, 5880–5887.
Xiao, C., & Fang, F. (2009). Ionic self-assembly and characterization of a polysaccharide-based polyelectrolyte complex of maleic starch half-ester acid with chitosan. *Journal of Applied Polymer Science, 112*, 2255–2260.
Yao, Z. L., Grishkewich, N., & Tam, K. C. (2013). Swelling and shear viscosity of stimuli-responsive colloidal systems. *Soft Matter, 9*, 5319–5335.
Yoo, S. H., & Jane, J. L. (2002). Molecular weights and gyration radii of amylopectins determined by high-performance size-exclusion chromatography equipped with multi-angle laser-light scattering and refractive index detectors. *Carbohydrate Polymers, 49*, 307–314.
Yusuf, A. A., Ayedun, H., & Logunleko, G. B. (2007). Functional properties of unmodified and modified Jack bean (*Canavalia ensiformis*) starches. *Nigerian Food Journal, 25*, 141–149.